SOIL ORGANISMS Volume 84 (2) 2012 pp. 431–443

ISSN: 1864-6417

A morphological comparison of two closely related ptychoid oribatid mite species: *Phthiracarus longulus* and *P. globosus* (Acari: Oribatida: Phthiracaroidea)

Sebastian Schmelzle[1]*, Roy A. Norton[2] and Michael Heethoff[1]

[1] *Universität Tübingen, Institut für Evolution und Ökologie, Abteilung Evolutionsbiologie der Invertebraten, Auf der Morgenstelle 28E, 72076 Tübingen, Germany*

[2] *State University of New York, College of Environmental Science and Forestry, 1 Forestry Drive, Syracuse NY 13210, USA*

** Corresponding author: Sebastian Schmelzle (e-mail: schmelzle@oribatida.com)*

Abstract

We studied exoskeletal and muscular adaptations to ptychoidy in the oribatid mite *Phthiracarus globosus* (Phthiracaridae, Phthiracaroidea) using synchrotron X-ray microtomography, and compared the results to *Phthiracarus longulus*, a closely related mite that we investigated earlier. As expected, both species show high similarity in most of the characters investigated, but there were also clear differences: the sensillus groove is more prominent and the bothridial scale is more angular in *P. globosus* than in *P. longulus*. The coxisternal retractor first found in *P. longulus* was also found in *P. globosus* and therefore could be a synapomorphy for the genus. The number of muscle fibres of the anterior dorsal endosternal muscle (ade), inferior prodorsal retractor (ipr), ventral plate adductor (vpa) and the notogaster lateral compressor (nlc) found in *P. globosus* is double or even triple that found in *P. longulus*. Our results suggest that muscle morphology might provide a phylogenetically informative set of characters for oribatid mite systematics, when more data are available.

Keywords: Synchrotron X-ray microtomography, SR-µCT, Ptychoidy, Phthiracaridae, Box mite, Predator defence

1. Introduction

Ptychoidy is the most complex morphological defensive mechanism in oribatid mites. It enables the mite to retract its legs and coxisternum into the idiosoma and encapsulate itself by deflecting the prodorsum ventrad as a seal (Sanders & Norton 2004). Ptychoidy appears to have independently evolved in three groups of the Oribatida: the Mesoplophoridae, Protoplophoridae and Ptyctima (Euptyctima in Weigmann 2006). All species of Ptyctima, consisting of the two superfamilies Phthiracaroidea and Euphthiracaroidea, are ptychoid as adults. The functional details of ptychoidy are best known for Euphthiracaroidea, with three species having been studied: *Euphthiracarus cooki* (Euphthiracaridae; Sanders & Norton 2004), *Rhysotritia ardua*, (Euphthiracaridae; Schmelzle et al. 2008, 2009) and *Oribotritia*

banksi (Oribotritiidae; Schmelzle et al. 2008, 2009). Similar information is available for only a single species of Phthiracaroidea: *Phthiracarus longulus* (C. L. Koch, 1841; Phthiracaridae; Schmelzle et al. 2010). These studies have shown clear differences between Euphthiracaroidea and Phthiracaroidea, such as a different organization of the ventral plates and their associated musculature (Schmelzle et al. 2010), and also noticeable differences within Euphthiracaroidea, which can be found in the fusion of the ventral plates and qualitative and quantitative muscle morphology (Euphthiracaridae and Oribotritiidae; Schmelzle et al. 2008, 2009). These findings suggest that muscle morphology might provide phylogenetically informative data for the Ptyctima, but closely related species must be investigated to determine the generality of similarities and homologies at a phylogenetically small scale. Hence, we investigated a second species of Phthiracaridae, *P. globosus* (C. L. Koch, 1841). We used synchrotron X-ray microtomography to show that the two closely related species are characterised by clear differences concerning exoskeletal and muscular characters that relate to ptychoidy.

2. Materials and Methods

Specimens: *Phthiracarus globosus* (synonyms: *P. globus* Parry, 1979; *P. gl*. Kamill, 1981; *Hoplophora globosa* Koch, 1841) is a Holarctic species of the family Phthiracaridae that is common and abundant in temperate forest litter (Niedbała 2002, Weigmann 2006). Adults for our studies (mean total length of 495 µm, n = 3, sd = 12.1) were collected from accumulated decaying needles and cone scales of introduced Norway spruce (*Picea abies*) in LaFayette, Onondaga Co., NY, USA.

Sample preparation: Specimens were killed and fixed in 1% glutaraldehyde for 60 h and stored in 70% ethanol. For the final preparation, specimens were dehydrated in an increasing ethanol series with steps of 70, 80, 90, 95 and 100%, with three changes at each step and 10 min between changes. After storage in fresh 100% ethanol they were critical-point dried in CO_2 (CPD 020, Balzers).

Scanning electron microscopy: Critical-point dried specimens were either glued onto a T-section-like metal foil or directly onto a stub and then sputter-coated with a 20 nm thick layer of gold or a gold-palladium mixture, respectively. Micrographs were taken on a Zeiss Evo LS10 scanning electron microscope at 10 keV and a Cambridge Stereoscan 250 Mk2 scanning electron microscope at 20 keV.

Synchrotron X-ray microtomography: Critical-point dried animals were fixed by the notogaster to the tip of a plastic pin (1.2 cm long; 3.0 mm diameter) using instant adhesive. Radiographs were taken at the European Synchrotron Radiation Facility (ESRF) in Grenoble at beamline ID19 with a beam energy of 20.5 keV and at a sample–detector distance of 20 mm. A cooled 14-bit CCD-camera with a resolution of 2048 x 2048 pixels and an effective pixel size of 0.7 µm per pixel was used (a detailed description of the method is given in Betz et al. 2007, Heethoff & Cloetens 2008, Heethoff et al. 2008). The data were visualized with the programs VGStudio MAX 1.2.1 (Volume Graphics, Heidelberg, Germany) and three-dimensional modeling of cuticular elements was conducted with amira™ 4.0.1 (Mercury Computer Systems Inc., Chelmsford, MA). Muscle fibres were counted using the original phase contrast microtomography data. Different portions of muscles are called muscle bands and subdivisions of muscle bands are called muscle fibres (Sanders & Norton 2004).

Tab. 1 Abbreviations, origin and insertion of the muscular elements associated with ptychoidy in *Phthiracarus globosus* and *P. longulus*.

Muscle	Abbr.	Origin	Insertion
Dorsoventral muscles of the prosoma			
coxisternal protractor	csp	notogaster, lateral	sejugal apodeme
coxisternal retractor	csr	notogaster, dorsal	apodeme 2 of the epimeres, apodemal shelves 3 and 4
inferior podosomal membrane adjustor	ima	anterior half of notogaster, ventrolateral	podosomal membrane
prodorsal dorsoventral muscle 1	pdv1	exobothridial field	lateral margin of apodemes 1
prodorsal dorsoventral muscle 2	pdv2	exobothridial field	lateral margin of apodemes 2
prodorsal dorsoventral muscle 3	pdv3	manubrial sclerite	sejugal apodeme
superior podosomal membrane adjustor	sma	notogaster, lateral	podosomal membrane
Endosternal division of the prosoma			
anterior dorsal endosternal muscle	ade	manubrial sclerite	endosternum
posterior dorsal endosternal muscle	pde	notogaster, dorsolateral	endosternum
subcapitulum endosternal retractor	ser	endosternum	mentum of subcapitulum
taenidiophore endosternal retractor	ter	endosternum	taenidiophore
Longitudinal division of the prosoma			
inferior prodorsal retractor	ipr	notogaster, dorsolateral	inferior retractor process, intercalary wall induration
prodorsum lateral adjustor	pla	notogaster, dorsolateral	manubrial sclerite
subcapitular retractor	scr	apodeme 1, 2 of the epimeres 1	anchoral process of subcapitular apodeme
superior prodorsal retractor	spr	notogaster, dorsal	basis of manubrial sclerite
Opisthosomal compressor system			
notogaster lateral compressor	nlc	notogaster, ventral curvature	anogenital membrane
ventral plate adductor	vpa	preanal apodeme	genital valve
ventral plate compressor	vpc	preanal apodeme	lateral edge of genital valve
Additional muscles			
postanal muscle	poam	terminal at posterior end of notogaster	postanal apodeme

3. Results and Discussion

Exoskeletal elements: *Phthiracarus globosus* is more spherical than *P. longulus*. This affects the notogaster, the prodorsum and the ventral plates, which are all broader and shorter than those of *P. longulus* (Figs 1–3).The interior and outer surfaces of the prodorsum of both species are homogeneously textured (Fig. 1). The sagittal apodeme is more prominent in *P. longulus* than in *P. globosus* (Figs 2b; 3b, c). The bothridial scale, covering the bothridium (Fig. 3a) is more rounded in *P. longulus* than in *P. globosus*. Phthiracarid mites do not possess a true manubrium like that of Euphthiracaroidea, i. e. an elongated posteroventral apodematal process of the prodorsum serving as an attachment structure for the origin and insertion of prodorsal retractors and adjustors (Sanders & Norton 2004, Schmelzle et al. 2008, 2009), despite our previous statement to that effect (Schmelzle et al. 2010). Instead, in both *Phthiracarus* species a manubrium-like sclerotized field lies within the articulating membrane adjacent to the posteroventral corner of the prodorsum (Fig. 3a, c, e) acting as functional manubrium: for this we use the term 'manubrial sclerite' (ms). The notogaster of *P. globosus* is more spherical and its cuticle is thicker (12–18 µm; Fig. 3d) than that of *P. longulus* (8–14 µm). Its anterior margin is separated into the lateral anterior tectum and the pronotal tectum by the tectonotal notch (Fig. 1a, b). Both allow for a tight connection of prodorsum and notogaster. The tectonotal notch exhibits a prominent sensillus groove (Fig. 3d) offering the sensillus (Fig. 1a, b) a place to rest and a scale receptacle (Fig. 3d) harbouring the bothridial scale whilst the animal is encapsulated. The sensillus groove is more pronounced in *P. globosus* than in *P. longulus*. This leads to a more defined position and less squeezing of the sensillus (Figs 1b, 3f) during encapsulation. At the ventral margin of the notogaster a medial ridge-like indentation is present (Fig. 1c) and also more pronounced in *P. globosus* than in *P. longulus*. This allows for a tight connection of ventral plates and notogaster in which the indentation (Fig. 1c) and the notch between the anal valves act according to the lock-and-key principle.

Thus, both phthiracarid species share the organisation of the ventral plates into distinct anal and genital valves, and also the manubrial sclerite. In these, they differ from most Euphthiracaroidea, which have a 'true' manubrium (a solid, cuticular process of the prodorsum) and elongated, bomb-bay like ventral plates, which may be fused in a variety of ways (Sanders & Norton 2004, Schmelzle et al. 2008). Of the exoskeletal elements that relate to ptychoidy, the two phthiracarid species differ in the shape of the bothridial scale, the size of the sagittal apodeme and the depth of the sensillus groove.

Muscular elements: In the following sections muscles will be addressed by their abbreviations only (cf. Tab. 1). The csp (dorsoventral muscles of the prosoma; Fig. 4b), originating laterally on the notogaster and inserting on the sejugal apodeme of the epimeres, can be found in both phthiracarid species but is not known in Euphthiracaroidea. The csp therefore might be a synapomorphic character for the genus *Phthiracarus* or even the Phthiracaroidea. Within the endosternal division of the prosoma the ade is the only muscle showing a noticeable difference between species: that of *P. longulus* consists of 2 muscle fibers while that of *P. globosus* consists of 5–6 muscle fibers (Fig. 5a). It originates at the endosternum and inserts on the manubrial sclerite in both species. The ipr originates dorsolaterally on the notogaster and inserts on the inferior retractor process and the intercalary wall induration of the prodorsum of both species, but the ipr of *P. globosus* (Fig. 6a) consists of almost twice the amount of muscle fibers seen in *P. longulus* (35–40 and 20–25 muscle fibers, respectively). The same is true for the spr: it consists of 4 muscle bands with 2 muscle fibers each in *P. globosus*

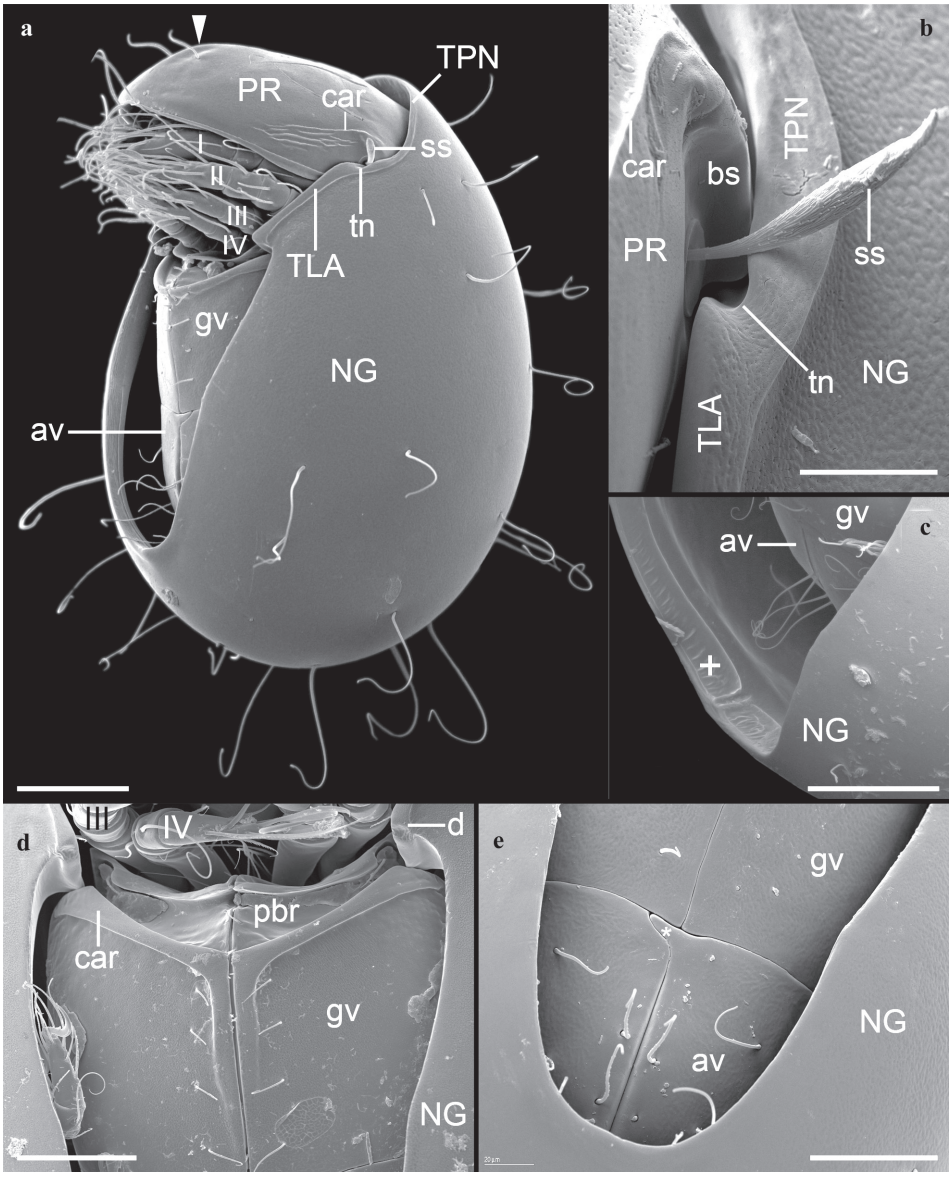

Fig. 1 *Phthiracarus globosus*. Scanning electron micrographs. **a**: Lateroventral overview of half encapsulated specimen (the withdrawn position of the ventral plates and the curled ends of notogastral setae are considered fixation artefacts; scale bar: 100 μm). **b**: Detail of the bothridial scale, the sensillus and the lateral anterior tectum (scale bar: 25 μm). **c**: Detail of the simple U-shaped ventral margin of the notogaster (scale bar: 100 μm). **d**: Detail of the articulation of the ventral plates and notogaster, the phragmatal bridge and ventral tooth (scale bar: 100 μm). **e**: Detail of the anterior anal lock (scale bar: 50 μm). Asterisk indicates the anterior lock of the anal plates, plus-symbol indicates the U-shaped plain lateral margin of the notogaster with a medial ridge-like indentation, arrowhead indicates the prodorsal ledge. (For abbreviations see in legend of Fig. 2).

(Fig. 6d) in comparison to 2–4 muscle fibers in *P. longulus,* even though both species are similar in size (495 µm and 540 µm, respectively). In both species, the spr originates dorsally on the notogaster and inserts on the basis of the manubrial sclerite. The nlc of *P. globosus* consists of 15–18 muscle bands with 1 or 2 muscle fibers each (Fig. 7a), whereas that of *P. longulus* consists of 3 muscle bands with 2 muscle fibers each and an additional portion of at least 5 muscle fibers. The nlc originates laterally on the notogaster and its insertion is restricted to the last third of the anogenital membrane (Fig. 7a). This corrects our previous statement about this muscle; portions 'nlc [c]' and 'nlc [d]' of Schmelzle et al. (2010) are in fact the retractors of the genital papillae (gpr), as already suspected by the authors. The vpa of *P. globosus* (Fig. 7b, c) has nearly twice the number of muscle fibers than that of *P. longulus* (10 muscle bands with 2–3 muscle fibers each and at least 12 muscle fibers, respectively; Fig. 7b, c), but in both species it originates on the preanal apodeme and inserts on the genital valve. The poam (originating terminally on the posterior end of the notogaster and inserting on the postanal apodeme) consists of 4–6 muscle bands with about 3–4 muscle fibers in *P. globosus* (Fig. 7d), compared to probably 4 muscle bands with a total of 10–15 muscle fibers in *P. longulus* (in contrast to Schmelzle et al. 2010), but the borders between the muscle bands seem to be less clear than in *P. globosus*.

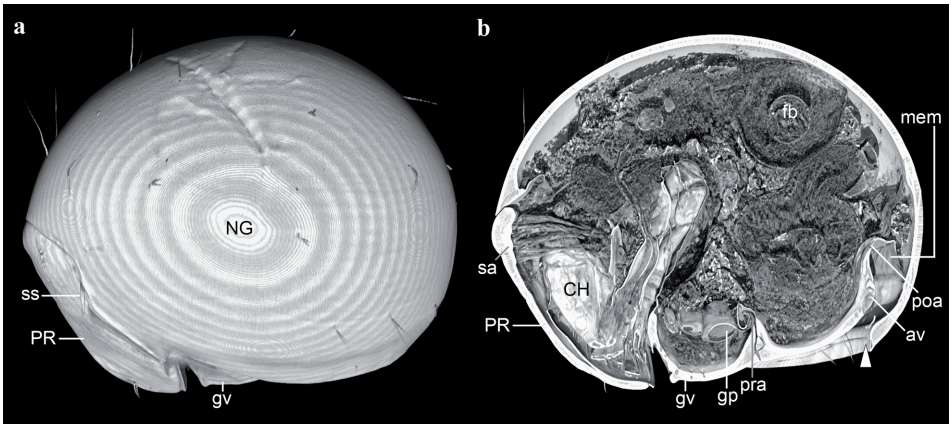

Fig. 2 *Phthiracarus globosus*, nearly encapsulated animal, lateral view. **a**: Overview of the animal (rendition of synchrotron X-ray microtomography data). **b**: Overview of a virtual sagittal section of a volume rendering of synchrotron X-ray microtomography data. Symbols: arrowhead indicates the U-shaped plain lateral margin of the notogaster.

Abbreviations: I–IV - walking legs 1–4, av - anal valve, bs - bothridial scale, car - carina, Ch - chelicera, csp - coxisternal protractor, csr - coxisternal retractor, d - ventral tooth of lateral anterior tectum, endo - endosternum, fb - food bolus, gp - genital papilla, gv - genital valve, ima - inferior membrane adjustor, irp - inferior retractor process, m - mentum of subcapitulum, mem - anogenital membrane, ms - manubrial sclerite, NG - notogaster, pbr - phragmatal bridge, pde - posterior dorsal endosternal muscle, ph - pharynx, PR - prodorsum, pra - preanal apodeme, poa - postanal apodeme, rl - rostral limb, RU - rutellum, sma - superior membrane adjustor, sa - sagittal apodeme, ser - subcapitulum endosternal retractor, sg - sensillus groove, sr - scale receptacle, ss - sensillus, ter - taenidiophore endosternal retractor, TLA - lateral anterior tectum, tn - tectonotal notch, tph - taenidiphore, TPN - pronotal tectum.

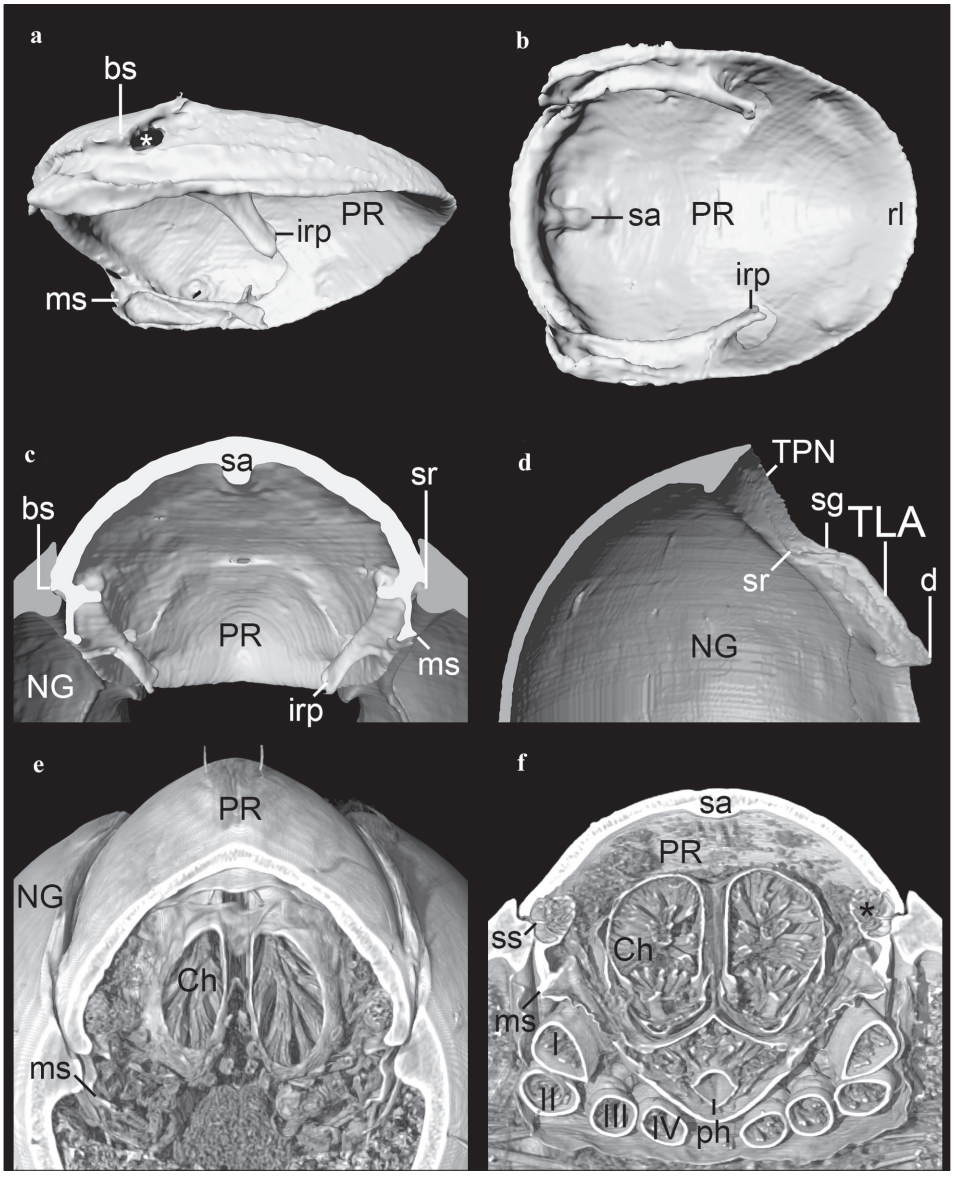

Fig. 3 *Phthiracarus globosus*, nearly encapsulated animal. Renderings of 3D-model (a–d) and volume rendering (e, f) of synchrotron X-ray microtomography data; c–f showing a dorsal view. **a**: Lateroventral view of the prodorsum. **b**: Ventral view of the prodorsum. **c**: Virtual frontal section in the region of the bothridial scale and its scale receptacle. **d**: Lateral view of virtual sagittal section showing the tectonotal notch with its scale receptacle and the sensillus groove. **e**: Virtual frontal section in the region of the manubrial sclerite. **f**: Virtual frontal section in the region of the opening of the bothridium. Asterisk in A and F indicates the location of the bothridium. (For abbreviations see in legend of Fig. 2)

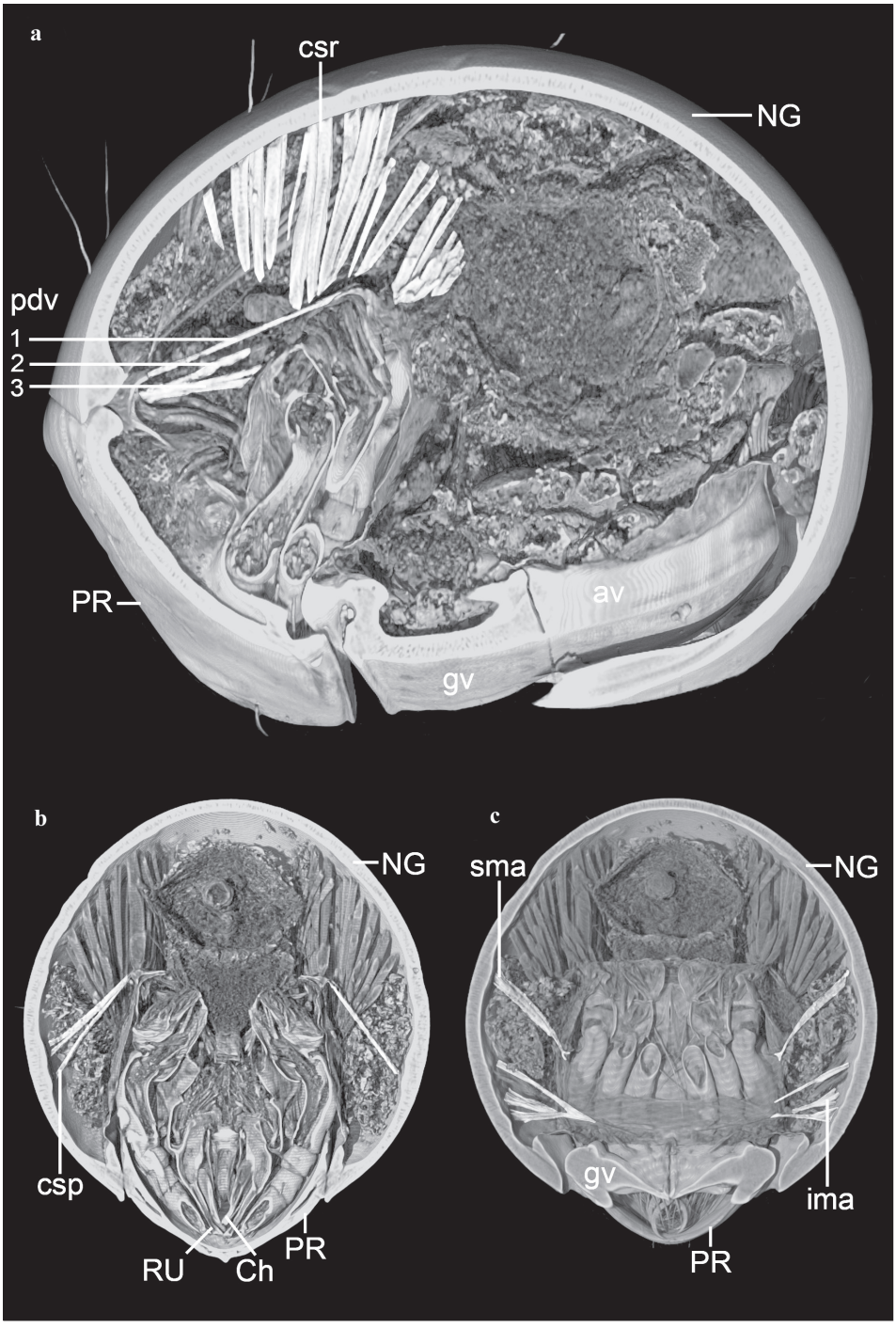
a
csr
NG
pdv
1
2
3
PR
av
gv
b
NG
csp
RU
Ch
PR
c
sma
NG
gv
ima
PR

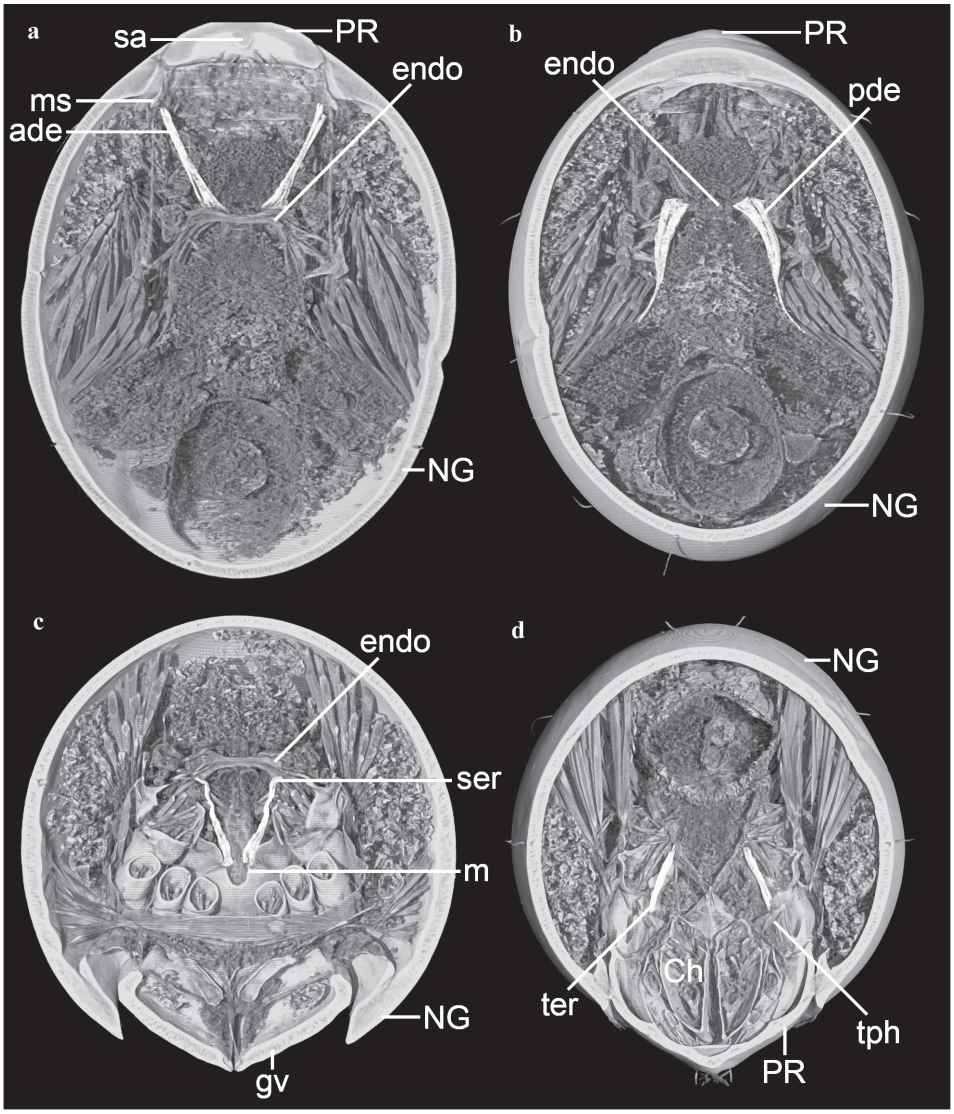

Fig. 5 *Phthiracarus globosus*, nearly encapsulated animal. Endosternal division of the prosoma. Volume renderings of synchrotron X-ray microtomography data. **a**: Dorsal view of virtual frontal section showing the anterior dorsal endosternal muscle (ade). **b**: Dorsal view of virtual frontal section showing the posterior dorsal endosternal muscle (pde). **c**: Virtual cross section showing the subcapitulum endosternal retractors (ser), posterior view. **d**: Virtual cross section showing the taenidiophore endosternal retractors (ter) , posterior view.

Fig. 4 (page 438) *Phthiracarus globosus*, nearly encapsulated animal. Dorsoventral muscles of the prosoma. Volume renderings of synchrotron X-ray microtomography data. **a**: Virtual sagittal section showing the coxisternal retractor (csr) and the prodorsal dorsoventral muscles 1–3 (pdv1–3) from lateral. **b**: Virtual cross section showing the coxisternal protractor (csp), posterior view. **c**: Virtual cross section showing the inferior (ima) and superior (sma) membrane adjustor, posterior view. (For all abbreviations see in legend of Fig. 2)

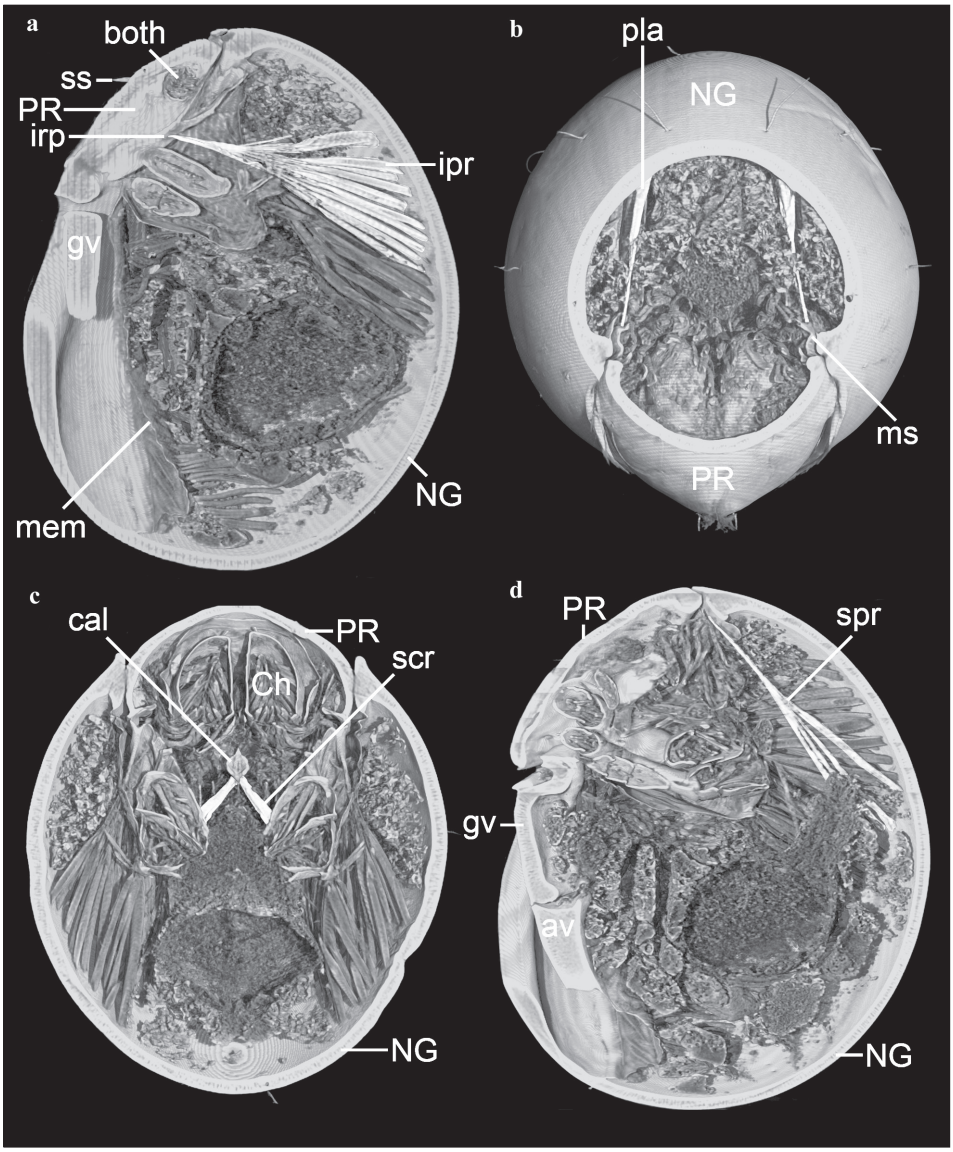

Fig. 6 *Phthiracarus globosus*, nearly encapsulated animal. Longitudinal division of the prosoma. Volume renderings of synchrotron X-ray microtomography data. **a**: Virtual sagittal section showing the inferior prodorsal retractors (ipr), lateral view. **b**: Anterior view of virtual cross section showing the prodorsum lateral adjustors (pla). **c**: Anterior view of virtual cross section showing the subcapitular retractor (scr). **d**: Virtual sagittal section showing the superior prodorsal retractors (spr), lateral view.

Abbr.: av - anal valve, both - bothridium, cal - lemniscus of the capitular apodeme, Ch - chelicera, gv - genital valve, ipr - inferior prodorsal retractor, irp - inferior retractor process, mem - anogenital membrane, ms - manubrial sclerite, NG - notogaster, pla - prodorsum lateral adjustor, PR - prodorsum, spr - superior prodorsal retractor, ss - sensillus.

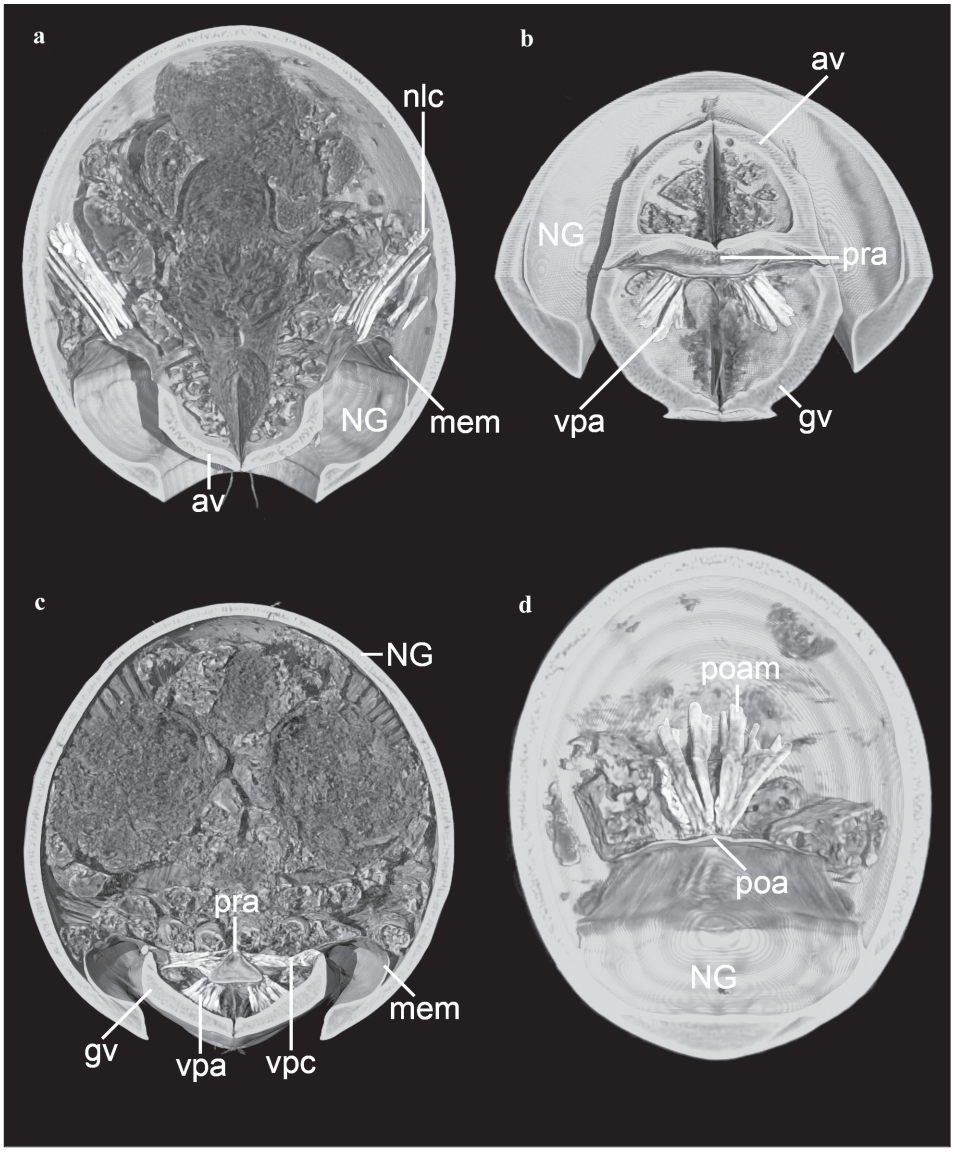

Fig. 7 *Phthiracarus globosus*, nearly encapsulated animal. Opisthosomal compressor system. Volume renderings of segmented synchrotron X-ray microtomography data. **a**: Anterior view on virtual cross section showing the notogaster lateral compressor (nlc). **b**: Combination of virtual cross and frontal section, anterodorsal view showing the ventral plate adductors (vpa). **c**: Virtual cross section showing the ventral plate adductors (vpa) and ventral plate compressors (vpc), viewing from anterior. **d**: Anterior view of virtual cross section showing the postanal muscle (poam).

Abbr.: av - anal valve, gv - genital valve, mem - anogenital membrane, NG - notogaster, nlc - notogaster lateral compressor, poa - postanal apodeme, poam - postanal muscle, pra - preanal apodeme, vpa - ventral plate adductor, vpc - ventral plate compressor.

4. Conclusions

Even though *Phthiracarus longulus* and *P. globosus* show a strong similarity, they clearly differ in some exoskeletal and muscular characters. The csp is present in *P. longulus* and *P. globosus* but so far in no euphthiracaroid mite. Further investigations of other genera (e.g. *Steganacarus*) and outgroups are necessary to possibly confirm the csp as a group synapomorphy of Phthiracaroidea. The number of bands/fibers observed for several muscles in *P. globosus* does not correlate with the size of the two species. In fact, the smaller *P. globosus* features double to triple the number of bands/fibers as were seen in *P. longulus* (ade, ipr, hva and nlc). We see no obvious reason for the difference, but suspect that the muscle volume might be more or less equal in the two species and just be distributed differently.

Most of the characters found in both species show a strong similarity and differences can only be found in the quality or quantity of certain, homologous characters (e.g. the depth of the sensillus groove and the number of muscle fibres of the ipr, respectively). By contrast, differences between the Phthiracaroidea and the Euphthircaroidea are at a larger scale, i. e, the presence or absence of complete features (e.g. the manubrium, the organisation of the ventral plates and the csp). Thus, informative signals of large phylogenetic scale can be found mainly in the presence or absence of characters, while those of small scale are found mostly in the quality or quantity of certain homologous features.

5. Acknowledgements

We thank Karl-Heinz Hellmer for the critical-point drying and Karl-Heinz Hellmer and Monika Meinert for taking the SEM micrographs. We thank Paavo Bergmann, Michael Laumann, Lukas Helfen and Peter Cloetens for their help with experiment SC-2127 at the ESRF in Grenoble and the European Synchrotron Radiation Facility for the allocated beam time. We thank the PRO ACAROLOGIA BASILIENSIS for funding the project.

6. References

Betz, O., U. Wegst, D. Weide, M. Heethoff, L. Helfen, W. K. Lee & P. Cloetens (2007): Imaging applications of synchrotron x-ray micro-tomography in biological morphology and biomaterial science. I. General aspects of the technique and its advantages in the analysis of arthropod structure.– Journal of Microscopy **22**: 51–71.

Heethoff, M. & P. Cloetens (2008): A comparison of synchrotron X-ray phase contrast tomography and holotomography for non-invasive investigations of the internal anatomy of mites. – Soil Organisms **80** (2): 205–215.

Heethoff, M., L. Helfen & P. Cloetens (2008): Non-invasive 3D-visualization of the internal organization of microarthropods using synchrotron X-ray-tomography with sub-micron resolution. – Journal of Visualized Experiments **15**: e737, DOI: 10.3791/737.

Niedbała, W. (2002): Ptyctimous mites (Acari, Oribatida) of the Nearctic Region. – Monographs of the Upper Silesian Museum, Bytom **4**: 1–261.

Sanders, F. H. & R. A. Norton (2004): Anatomy and function of the ptychoid defensive mechanism in the mite *Euphthiracarus cooki* (Acari: Oribatida). – Journal of Morphology **259**: 119–154.

Schmelzle, S., L. Helfen, R. A. Norton & M. Heethoff (2008): The ptychoid defensive mechanism in Euphthiracaroidea (Acari: Oribatida): A comparison of exoskeletal elements. – Soil Organisms **80** (2): 227–241.

Schmelzle, S., L. Helfen, R. A. Norton & M. Heethoff (2009): The ptychoid defensive mechanism in Euphthiracaroidea (Acari: Oribatida): A comparison of muscular elements with functional considerations. – Arthropod Structure and Development **38** (6): 461–472.

Schmelzle, S., L. Helfen, R. A. Norton & M. Heethoff (2010): The ptychoid defensive mechanism in *Phthiracarus longulus* (Acari, Oribatida, Phthiracaroidea): Exoskeletal and muscular elements. – Soil Organisms **82** (2): 253–273.

Weigmann, G. (2006): Hornmilben (Oribatida). – Goecke & Evers, Keltern: 520 pp.

Accepted 26 March 2012